

## Flaw Generation by Indentation in Glass Fibers

T. P. DABBS, D. B. MARSHALL, and B. R. LAWN\*

THE ultimate practicality of glass fibers as optical waveguides in the communications industry will depend on the ability to manufacture and maintain long lengths (>1 km) free of large flaws. It is now recognized that extraneous stress-concentrating agents, notably dust particles, constitute a prime source of such flaws, during both forming and subsequent handling.<sup>1</sup> To cope with the formidable task of predicting survival rates over the extreme lengths required, resort is most generally made to statistical methods for characterizing the flaw populations; the usual approach is to measure strengths of a large number of short-length specimens ( $\approx 1$  m), and extrapolate the data in accordance with a Weibull distribution function.<sup>2-5</sup> Typically, the short-length strengths are variable, falling within a range  $\approx 0.2$  to 6 GPa (corresponding to penny-like-flaw sizes  $\approx 10$  to  $0.01 \mu\text{m}$ ), with a tendency to a bimodal distribution. However, while quantitative information of this type is useful for predictive purposes, it provides no physical insight into the actual stress-concentration processes responsible for flaw generation. These processes need to be identified<sup>6</sup> and understood if fiber design is to be placed on a sound, fundamental footing.

In this work an indentation fracture technique is used to simulate the conditions under which flaws are produced. The essential stress concentration arises directly from mechanical loading of an appropriate sharp indenter on the fiber surface. "Real" concentration mechanisms may have a quite different origin (e.g. differential thermal expansion between an embedded foreign particle and its matrix), but the indentation procedure offers a particularly simple means of quantifying the severity of flaws in terms of a measurable driving force. Moreover, events beneath a loaded indenter are amenable to direct, microscopic observation.<sup>7</sup>

Silica glass fibers were fabricated\* by a standard chemical vapor deposition procedure. The fibers were drawn to a diameter of  $\approx 135 \mu\text{m}$  and consisted of a core with 12%  $\text{P}_2\text{O}_5$ , a cladding with 10%  $\text{B}_2\text{O}_3$ , and a jacket with 4%  $\text{B}_2\text{O}_3$ . A silicone resin coating<sup>†</sup> was applied during the drawing. Specimens (0.5 m long) were prepared for testing by removing a small central portion of coating; removal was effected by dissolving the resin in concentrated sulfuric acid, after which the fiber was rinsed in water and dried carefully with a tissue. Examination of the fibers in polarized light showed little birefringence, indicating negligible residual stresses at the interfacial boundaries.

Each newly prepared fiber was subjected to an indentation procedure. Individual specimens were mounted in thermosetting wax onto a jig which allowed in situ observations of the entire contact cycle.<sup>7</sup> Viewing was done through an inverted microscope, with the jig seated on a translation stage. This setup enabled the contact axis to be accurately aligned along a fiber diameter, at some preselected position along the length. A Vickers diamond pyramid was used to indent the specimen surface. The working range of loads was 0.1 to 1.0 N: the lower load represented the limit of the microhardness testing equipment; above the upper load the fibers shattered. All indentation tests were conducted in air, with the peak load maintained for  $\approx 7$  s. The indentation pattern showed the classical features typical of brittle solids<sup>6,8</sup>: (1) a square, irreversible impression, with the half-diagonal  $a$  characterizing the deformation response of the material, and (2) above a threshold in the loading<sup>9</sup> (which varied considerably over the available range), well-defined

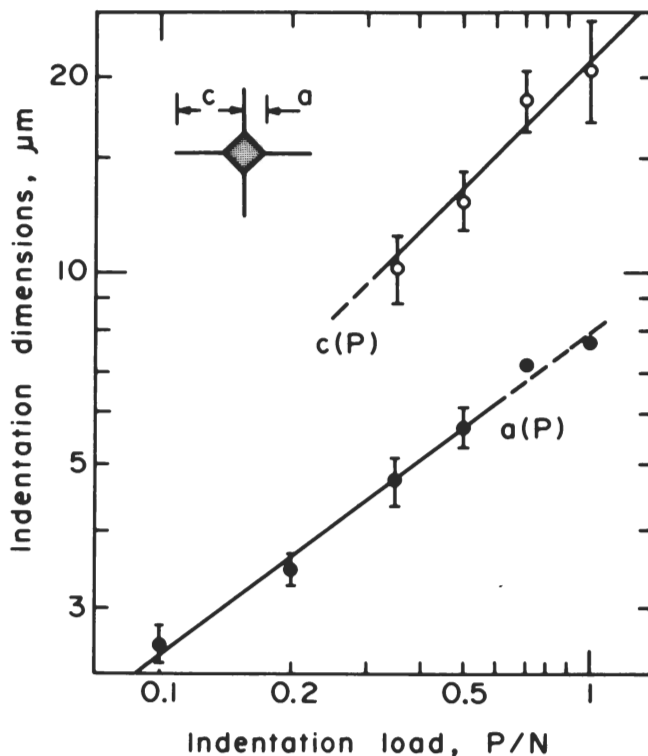


Fig. 1. Characteristic indentation dimensions as function of load for fused silica fibers. Fracture data,  $c(P)$ , taken from indentations with well-developed radial cracks, deformation data,  $a(P)$ , from indentations without such cracks. The threshold region is evident. Data points with error bars represent mean and standard deviation for 4 to 11 indentations.

radial cracks extending from the impression corners, with the mean radius  $c$  accordingly characterizing the fracture response. In all cases the indentation cracks were wholly contained within the jacket layer. Figure 1 shows the measured characteristic dimensions as a function of indentation load  $P$ . The curves fitted to the data are of the standard forms  $P/a^2 \sim H$  and  $P/c^{3/2} \sim K_c$ ,<sup>8</sup> where hardness  $H$  and toughness  $K_c$  are material constants used in quantifying the general deformation/fracture response.<sup>10</sup>

The indented fibers were broken using circular end clamps to ensure essential tensile loading. A stressing rate of  $7.5 \text{ MPa s}^{-1}$  was used in all tests. Kinetic effects were kept to a minimum in the strength evaluation by covering the contact site with paraffin oil immediately prior to clamping. The broken ends of the fibers were examined microscopically to determine whether or not failure had originated at the indentation; negative results were rejected. The strength data are shown in Fig. 2 as a function of indentation load. Two distinct groups of data are observed, corresponding to impressions with and without well-developed radial cracks. The curves are representations of the indentation/strength relation  $\sigma P^{1/3} \sim K_c^{4/3}$ ,<sup>11</sup> obtained by substituting  $c \propto (P/K_c)^{2/3}$  into the standard strength equation  $\sigma \sim K_c/c^{1/2}$ ; the lower curve is an extrapolation of results from control strength tests on bulk glass rods of composition close to that of the fiber jacket (6 rods, indentation load  $P = 100$  N, failure stress  $\sigma = 34.8 \pm 2.0 \text{ MPa}$ )<sup>12</sup>; the upper curve is a simple data fit.

It is evident from Fig. 2 that fiber strength degrades systematically with severity of contact, with a clear change in mechanism at the radial cracking threshold. Above the threshold the degradation mechanism is well defined; the radial cracks have propagated well out from the central deformation zone, and accordingly satisfy

Received September 17, 1979; revised copy received October 25, 1979.

The writers are with the Department of Applied Physics, School of Physics, University of New South Wales, Kensington, New South Wales 2033, Australia.

\*Member, the American Ceramic Society.

†At Amalgamated Wireless, Australasia.

†GERTV 670.

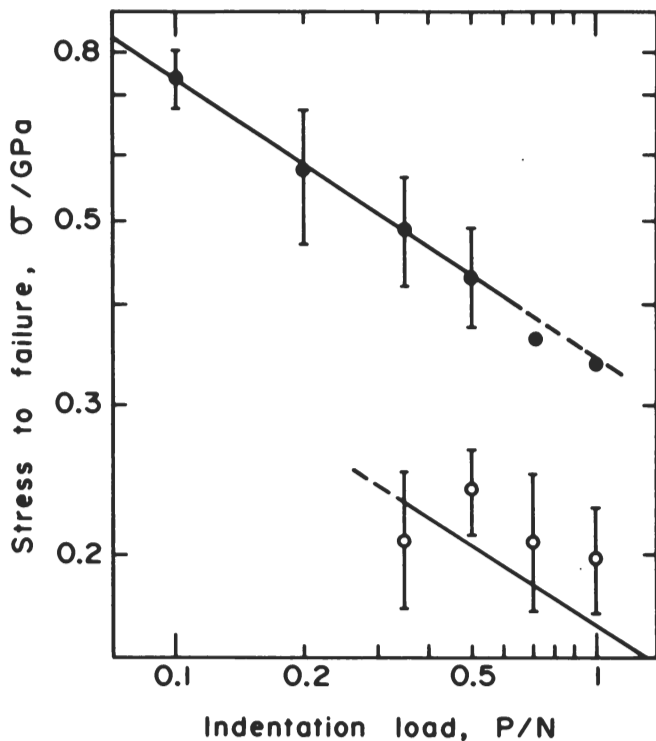


Fig. 2. Strength of fibers indented as in Fig. 1. Note abrupt decrease in strength as the threshold load for radial cracking is exceeded.

simple fracture mechanics relations (such as that represented in Fig. 1) for idealized crack geometries. However, below the threshold the mechanism is more obscure. Since  $\sigma \propto c^{-1/2}$ , the abrupt increase in strength by a factor of  $\approx 2$  in going from the lower to the upper curve in Fig. 2 corresponds to a decrease by a factor of  $\approx 4$  in flaw size; a reduction on this scale takes us into the region  $c < a$  in Fig. 1, i.e. the degrading flaws are fully encompassed within the hardness impression. Close microscopic examination of the damage zone beneath the contact site shows a complex network of incipient flaws associated with a highly disruptive flow process.<sup>13,14</sup> The crack problem now falls within the realm of nucleation,<sup>15</sup> where all the complications of elastic/plastic stress fields, flaw/flaw interactions, etc. need to be taken into account. Despite these complications, the subthreshold response is of special interest, for it is in this region that the strengths in Fig. 2 begin to approach those of as-received fibers. An extension of the data to the theoretical strength limit,  $\approx 6$  GPa, using microcontact techniques<sup>16</sup> capable of delivering loads down to  $\approx 10$  mN (extrapolation of upper curve in Fig. 2) and truly pristine fibers, might accordingly be expected to provide information on the nature of flaws at the lower end of the size spectrum. On the other hand, the range of the present results should be sufficient to emphasize caution in applying macroscopic crack data to predict microscopic flaw behavior; the failure of conventionally determined crack-velocity data to account for fatigue properties of freshly drawn fibers is a case in point.<sup>17</sup>

<sup>1</sup>R. D. Maurer, "Effect of Dust on Glass Fiber Strength," *Appl. Phys. Lett.*, **30** [2] 82-84 (1977).

<sup>2</sup>R. D. Maurer, "Strength of Fiber Optical Waveguides," *ibid.*, **27** [4] 220-21 (1975).

<sup>3</sup>C. R. Kurkjian, R. V. Albarino, J. T. Krause, H. N. Vazirani, F. V. DiMarcello, S. Torza, and H. Schonhorn, "Strength of 0.04-50 m Lengths of Coated Fused Silica Fibers," *ibid.*, **28** [10] 588-90 (1976).

<sup>4(a)</sup>B. K. Taryyal and D. Kalish, "Application of Weibull-Type Analysis to the Strength of Optical Fibers," *Mater. Sci. Eng.*, **27** [1] 69-71 (1977).

<sup>4(b)</sup>B. K. Taryyal and D. Kalish, pp. 161-75 in *Fracture Mechanics of Ceramics*, Vol. 3. Edited by R. C. Bradt, D. P. H. Hasselman, and F. F. Lange. Plenum, New York, 1978.

<sup>5</sup>W. E. Snowden, pp. 143-59 in Ref. 4(b).

<sup>6</sup>B. R. Lawn and T. R. Wilshaw, "Indentation Fracture: Principles and Applications," *J. Mater. Sci.*, **10** [6] 1049-81 (1975).

<sup>7</sup>V. R. Howes, "Surface Strength of Coated Glass," *Glass Technol.*, **15** [6] 148-52 (1974).

<sup>8</sup>B. R. Lawn, T. Jensen, and A. Arora, "Brittleness as an Indentation Size Effect," *J. Mater. Sci.*, **11** [3] 573-75 (1976).

<sup>9</sup>B. R. Lawn and A. G. Evans, "Model for Crack Initiation in Elastic/Plastic Indentation Fields," *ibid.*, **12** [11] 2195-99 (1977).

<sup>10</sup>B. R. Lawn and D. B. Marshall, "Hardness, Toughness, and Brittleness: An Indentation Analysis," *J. Am. Ceram. Soc.*, **62** [7-8] 347-50 (1979).

<sup>11</sup>B. R. Lawn and D. B. Marshall, pp. 205-29 in Ref. 4(b).

<sup>12</sup>P. Chantikul, D. B. Marshall, B. R. Lawn, and M. G. Drexhage, "Contact-Damage Resistance of Partially Leached Glasses," *J. Am. Ceram. Soc.*, **62** [11-12] 551-55 (1979).

<sup>13</sup>J. T. Hagan and M. V. Swain, "Origin of Median and Lateral Cracks Around Plastic Indents in Brittle Materials," *J. Phys. D.*, **11** [15] 2091-2102 (1978).

<sup>14</sup>A. Arora, D. B. Marshall, B. R. Lawn, and M. V. Swain, "Indentation Deformation/Fracture of Normal and Anomalous Glasses," *J. Non-Cryst. Solids*, **31** [3] 915-28 (1979).

<sup>15</sup>B. R. Lawn and T. R. Wilshaw, *Fracture of Brittle Solids*; Ch. 2. Cambridge University Press, London, 1975.

<sup>16(a)</sup>N. H. Macmillan and F. P. Bowden, "Microdeformation of Solids," *J. Appl. Phys.*, **39** [3] 1432-35 (1968).

<sup>16(b)</sup>N. H. Macmillan and N. H. Macmillan, "Microdeformation of Solids," *ibid.*, **41** [2] 672-73 (1970).

<sup>17</sup>J. E. Ritter, Jr. and K. Jakus, "Applicability of Crack Velocity Data to Lifetime Predictions for Fused Silica Fibers," *J. Am. Ceram. Soc.*, **60** [3-4] 171 (1977).